PONTIFICIA UNIVERSIDAD CATÓLICA DEL PERÚ

ESCUELA DE POSGRADO

Topological phases generated with single photons entangled in polarization and momentum

A thesis in candidacy for the degree of Master of Science in Physics
presented by:

Elmer Eduardo Suarez Yana

Advisor:
Prof. Francisco de Zela

Jury:
Prof. Eduardo Massoni
Prof. Hernán Castillo

Lima, 2016

Topological phases generated with single photons entangled in polarization and momentum

Elmer Eduardo Suarez Yana

Propuesto para el grado de Magíster en Física

Resumen

El entrelazamiento puede abordarse desde dos perspectivas diferentes: como un recurso esencial para las tecnologías cuánticas y como un fenómeno fundamental que está íntimamente relacionado con nuestra comprensión de la naturaleza misma. Por otro lado, la teoría cuántica se formula en el marco teórico de los espacios de Hilbert, para los que el entrelazamiento juega un papel importante en la determinación de su geometría y topología. Las características topológicas que puedan exhibirse al utilizar estados entrelazados son largamente independientes de la realización física particular del entrelazamiento: puede afectar a un solo grado de libertad poseido por dos partículas diferentes, o bien puede implicar dos grados diferentes de libertad que se cohesionan a una misma partícula o entidad física, por ejemplo, un campo electromagnético. Resulta que la manipulación de los grados de libertad de polarización y momentum (camino) ya sea de forma independiente el uno del otro o mediante la aplicación de evoluciones unitarias no separables es muy versátil. Con esto en mente, la presente tesis apunta hacia el diseño e implementación de arreglos experimentales que se pueden utilizar para estudiar fases geométricas y topológicas en sistemas de dos qubits mediante el uso de los grados de libertad de momentum (camino) y polarización de un solo fotoón. Finalmente mostramos el diseño de un experimento, apuntado a exhibir la fase topológica, y los resultados obtenidos.

Topological phases generated with single photons entangled in polarization and momentum

Elmer Eduardo Suarez Yana

Presented Towards a Master's Degree in Physics

Abstract

Entanglement can be addressed from two different perspectives, namely as an essential resource for quantum technologies and as a fundamental phenomenon that is intimately related to our understanding of Nature itself. On the other hand, quantum theory is formulated within the mathematical framework of Hilbert spaces, for which entanglement plays an important role in the determination of their geometry and topology. The topological features that can be exhibited when using entangled states are largely independent of the particular physical realization of entanglement: it can involve a single degree of freedom carried along by two different particles, or else it can involve two different degrees of freedom that are attached to one and the same particle or physical entity, e.g., an electromagnetic field. Turns out that the manipulation of polarization and momentum (path) degrees of freedom either independently from one another or by applying non-separable unitary evolutions to product or to entangled initial states is very versatile. With this in mind, the present thesis points towards the design and implementation of experimental arrays that can be used to exhibit geometric and topological phases in two-partite systems by using polarization and momentum (path) degrees of freedom. Finally, we show the design of an experiment aimed to exhibit topological phases and the results obtained.

Acknowledgments

The realization of this work could not have been possible without the investment of time and patience of some people. First, my mom and my sister who have helped me, replacing me, in many niggling things at home that, in total, sum up a lot of extra time and less stress for me. Also, to friends and partners that sometimes took care of softenig hard days.

The realization of the experiment is a team work for which I thank specially Omar Ortiz and Yonny Yugra who helped me even at the border of giving up, when any crazy idea was permissible.

I owe a lot to my teacher Francisco de Zela specially for his support in this hard, stressful 3 months. I owe Eduardo Massoni too for encouraging me from the very beginning in his highly pragmatic ways.

For the scholarship I thank Concytec. This will help me take more chances.

Contents

Chapter 1

Introduction

Quantum mechanics is the ultimate theory in physics. As it was to be expected, new technology was developed and continues to be under the paradigm of quantum information or microelectronics; however, it has also been useful in the pursuit of a deeper understanding of nature. The present work is intended in the latter sense, since we address fundamental issues that concern the topology and/or geometry underlying the evolution of a quantum state. In order to do this we design experimental arrays that can be used to exhibit geometric and topological phases in bipartite systems [1]. By taking advantage of the versatility of the array proposed by Englert et al. [2] we aim to fully exploit its capabilities that allow us to manipulate polarization and momentum degrees of freedom of single photons. At the end, we show the design and final results obtained for one particular array with the objective of exhibiting topological phases.

Previous research has been done along the above lines: Loredo et al. [3] measured the geometric and topological phase of two entangled photons, Souza et al. [4, 5] measured the topological phase in vortex beams and J. Du et al. [6] measured topological phases using a pair of nuclear spins.

We shall now briefly discuss basic concepts that will be used in this thesis work.

1.1 The quantum bit

In electronics and information science the basic unit of information is the bit. The bit represents a dichotomy, that is, it describes systems with only two possible states and is commonly written as 0 or 1. As an example, a light bulb may only be on or off.

In the quantum regime, a bit falls short trying to represent any state of a two dimensional system; it lacks the ability to be in a superposition. A qubit does not;

indeed, it is defined as

$$|\Psi\rangle = a_0 |0\rangle + a_1 |1\rangle \tag{1.1}$$

with $|a_0|^2 + |a_1|^2 = 1, a_0, a_1 \in \mathbb{C}$. This is a pure state of a two dimensional quantum system. In formal words, it is a vector in a Hilbert space $\mathcal{H}$ with an orthonormal basis $\{|0\rangle, |1\rangle\}$ usually called the computational or standard basis.

A photon has three degrees of freedom which are of common use in quantum optics: polarization, angular momentum and linear momentum. For the present work two qubits will be of use: polarization and linear momentum.

1.1.1 Polarization as a qubit

Polarization is part of the description of light by Maxwell's equations. In absence of free charges, the complex electric field is a two dimensional vector describing a plane-wave beam propagating along some direction ($\vec{k}$):

$$\vec{E} = (E_1 e^{i\varphi_1} \hat{e}_1 + E_2 e^{i\varphi_2} \hat{e}_2) e^{i(\vec{k}\cdot\vec{r} - \omega t)} \tag{1.2}$$

with $E^2 = E_1^2 + E_2^2$ and a pair of perpendicular, in general complex, unit vectors $\{\hat{e}_1, \hat{e}_2\}$.
We reparametrize by making $\cos\theta = E_1/E$, $\sin\theta = E_2/E$ to obtain:

$$\vec{E} = (e^{i\varphi_1} \cos\theta \hat{e}_1 + e^{i\varphi_2} \sin\theta \hat{e}_2) E e^{-i(\vec{k}\cdot\vec{r} - \omega t)} \tag{1.3}$$

From this we can extract the so called fundamental vector mode function; by omitting the global $e^{-i(\vec{k}\cdot\vec{r} - \omega t)}$ phase for the moment, we obtain

$$\hat{E} = e^{i\varphi_1} \cos\theta \hat{e}_1 + e^{i\varphi_2} \sin\theta \hat{e}_2 \tag{1.4}$$

Which we may call the unit vector of polarization.

This representation is not suitable for describing the particle nature of light: photons. Photons are a consequence of the quantization of the EM field, and are represented by Fock states. Any given Fock state pertains to a mode specified by $\vec{k}$ and one of the two polarization basis vectors tagged by $s = 1, 2$. A single photon with a fixed $\vec{k}$ can ocuppy two modes: $|1\rangle_{\vec{k},s=1}$ and $|1\rangle_{\vec{k},s=2}$. These states can form a qubit and are usually rewritten as

$$|\Psi\rangle = e^{i\varphi_1} \cos\theta |H\rangle + e^{i\varphi_2} \sin\theta |V\rangle \tag{1.5}$$

where $|H\rangle(|V\rangle)$ is a shorthand notation for $|1\rangle_{\vec{k},s=1}(|1\rangle_{\vec{k},s=2})$ and refer to a horizontal

and vertical direction respectively. This can be seen as the unit vector of polarization written in Dirac's notation with a particular choice of basis.

1.1.2 Linear momentum as a qubit

Linear momentum is parallel to the wave vector. Indeed, in the classical approach $\vec{p} = \epsilon \frac{E^2}{\omega_{\vec{k}}} \vec{k}$. While in the quantum approach the momentum operator $\hat{P} = \sum_{\vec{k},s} \hbar \vec{k} a^\dagger a$ i.e., $|n\rangle_{\vec{k},s}$ is and eigenvector for the eigenvalue $n\hbar\vec{k}$ of the momentum operator $\hat{P}$. Usual notation involves $\vec{k}$ instead, for this reason we omit writing $\vec{p}$ in the following paragraphs.

An EM wave incident in a material may be reflected, transmitted or absorbed. Details depend on the particular material or on the incident polarization but, most important is to notice the similarity to the polarization case:

$$\vec{E}_{out} = (te^{i(\vec{k}_t \cdot \vec{r})} + re^{i(\vec{k}_r \cdot \vec{r})})\vec{E}_{in} \tag{1.6}$$

Where t and r are the transmission and reflection coefficient respectively. We have two waves going in different directions ($\vec{k}_r$ and $\vec{k}_t$); while with polarization we have a vector with two possible directions ($\vec{e}_1$ and $\vec{e}_2$).

For the single photon case, we must rephrase this by saying that it can excite only two modes after passing through the material: $|1\rangle_{\vec{k}_r,\Psi_R}$ and $|1\rangle_{\vec{k}_t,\Psi_T}$. In general, the polarization states for each $\vec{k}$ ($|\Psi_R\rangle$ and $|\Psi_T\rangle$) are not necessarily perpendicular nor parallel but for the present work we shall consider the ideal case where polarization is not changed and the reflecting materials do not absorb light. In this case we may rewrite the state as:

$$|out\rangle = t\,|T\rangle + r\,|R\rangle \tag{1.7}$$

where the coefficients depend on the material only, $|t|^2 + |r|^2 = 1$ and polarization remains unchanged.

1.2 Qubit transformation

The evolution or transformation of a closed system is described by a unitary operator. Being a qubit a state of a closed two dimensional system its unitary evolution must be described by an element of the $U(2)$ group. However, we shall focus on those with determinant equal to one which form a subgroup called $SU(2)$. This is because we are not interested in global phases, such as distinguishing $U(2)$ from $SU(2)$ elements.

Let α and β be two complex numbers such that $|\alpha|^2 + |\beta|^2 = 1$. The matrix representation of any $SU(2)$ can be written as

$$U = \begin{pmatrix} \alpha & -\beta^* \\ \beta & \alpha^* \end{pmatrix}. \tag{1.8}$$

We can parametrize $SU(2)$ by making use of the operator basis, this consists of the Pauli matrices σ_1, σ_2 and σ_3 and the unit operator $\mathbb{1}$. There are three ways this can be done

1. **Homogeneous Euler angle parametrization**

   It depends on 4 variables (a_0, a_1, a_2, a_3) with the constraint $a_0^2+a_1^2+a_0^2+a_3^2 = 1$, written as

   $$U = a_0\mathbb{1} - i\vec{a}\cdot\vec{\sigma} \tag{1.9}$$

   where $\vec{\sigma}$ denotes the triple of Pauli matrices.

2. **Axis-angle parametrization**

   It depends on the coordinates of a unitary vector $\hat{n} = (n_1, n_2, n_3)$ and a rotation α, written as

   $$U = e^{-i\alpha\hat{n}\cdot\vec{\sigma}} = \cos\alpha\mathbb{1} - i\sin\alpha\hat{n}\cdot\vec{\sigma} \tag{1.10}$$

3. **Euler angle parametrization**

   It depends on 3 angles (ξ, η, ζ), written as

   $$U = exp(-i\xi\sigma_2/2)exp(-i\eta\sigma_3/2)exp(-i\zeta\sigma_2/2) \tag{1.11}$$

We will now explain how this type of evolutions are implemented in the qubits of polarization and momentum.

1.2.1 Polarization transformation

Birefringent materials are commonly used to change polarization. This materials have two indices of refraction, η_1 and η_2, each one oriented along one of two mutually perpendicular directions. If $\eta_1 > \eta_2$ say, we then refer to the η_2 direction as fast axis and the η_1 direction as slow axis.

The crystal coordinate system defines two preferred axis along which an incident wave or photon accumulates different phases. The matrix representation of the

$SU(2)$ operator describing this transformation is

$$U_{Bf} = \begin{pmatrix} e^{i\phi} & 0 \\ 0 & e^{-i\phi} \end{pmatrix} \tag{1.12}$$

using the $\{fast, slow\}$ basis and ϕ depends on the length and type of material as well as the wavelength. Two cases are of great importance: the quarter wave plate ($\phi = \pi/4$) and the half wave plate ($\phi = \pi/2$).

Polarization can be defined with respect to a coordinate system that may be misaligned with respect to the crystal's system. The laboratory coordinate system defined by the horizontal and vertical direction, $|H\rangle$ and $|V\rangle$, is our fixed reference system; we must apply to 1.12 a change of basis. Let the fast axis make an angle θ with the horizontal direction, then the rotation matrix is given by

$$R(\theta) = \begin{pmatrix} \cos\theta & -\sin\theta \\ \sin\theta & \cos\theta \end{pmatrix}. \tag{1.13}$$

Applying this rotation to the quarter and half wave plate cases (see Eq. (1.12) with $\phi = \pi/4$ and $\pi/2$, respectively) we obtain

$$Q(\theta) = \frac{1}{\sqrt{2}} \begin{pmatrix} 1 + i\cos(2\theta) & i\sin(2\theta) \\ i\sin(2\theta) & 1 - i\cos(2\theta) \end{pmatrix} \tag{1.14}$$

and

$$H(\theta) = i \begin{pmatrix} \cos(2\theta) & \sin(2\theta) \\ \sin(2\theta) & -\cos(2\theta) \end{pmatrix}. \tag{1.15}$$

Where Q and H refers to quarter and half wave plate respectively.

A set of only two quarters and one half wave plate are necessary and sufficient to realize an $SU(2)$ operator [7]. It turns out that there is a linear relation between the parameters of 1.11 and the angles the plates must be rotated:

$$U(\xi, \eta, \zeta) = Q_{(\pi/4+\xi/2)} H_{(-\pi/4+\frac{\xi+\eta-\zeta}{4})} Q_{(\pi/4-\zeta/2)}. \tag{1.16}$$

We take the convention of writing at far right the first plate into which the light is incident.

Some properties will be of use later on:

- Quarter and Half may be interchanged

$$Q_{(\alpha)} H_{(\beta)} = H_{(\beta)} Q_{(2\beta-\alpha)} \tag{1.17}$$

- An extra Half may be absorbed

$$Q_{(\alpha)}H_{(\beta)}H_{(\gamma)} = Q_{(\alpha+\pi/2)}H_{(\alpha-\beta+\gamma-\pi/2)}. \tag{1.18}$$

- Two ways to write any plate

$$H_{(\alpha)} = H_{(\alpha+\pi)} \quad Q_{(\alpha)} = Q_{(\alpha+\pi)} \tag{1.19}$$

- Inverse of any plate

$$H_{(\alpha)}^{-1} = H_{(\alpha+\pi/2)} \quad Q_{(\alpha)}^{-1} = Q_{(\alpha+\pi/2)} \tag{1.20}$$

1.2.2 Momentum transformation

How much of a wave is reflected or transmitted can be controlled by using a beam splitter (BS). This consist of a partially reflecting mirror specially engineered to reflect, for a fixed range of wavelengths, a certain percentage of the incident wave power. Up to this point it is ambiguous how we should define the phases of the t and r coefficients in 1.7. To deal with this we will assume symmetric beam splitters in the ideal case. The matrix representation of the $SU(2)$ operator associated with this device would be

$$\begin{pmatrix} \cos\theta & i\sin\theta \\ i\sin\theta & \cos\theta \end{pmatrix}. \tag{1.21}$$

where the first and second column correspond to the action over light incident in the $\vec{k}_1$ and $\vec{k}_2$ direction respectively (Figure 1.1) and $\cot^2\theta$ is the transmitted:reflected power ratio.

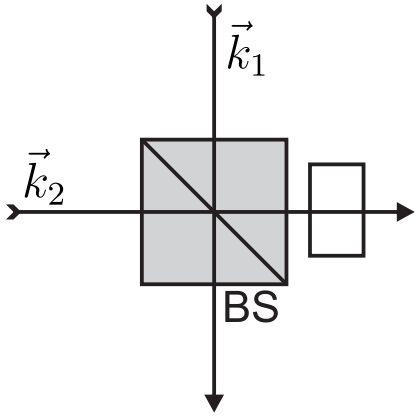

Figure 1.1: An ideal, symmetric, cube beam splitter with a black space at one end.

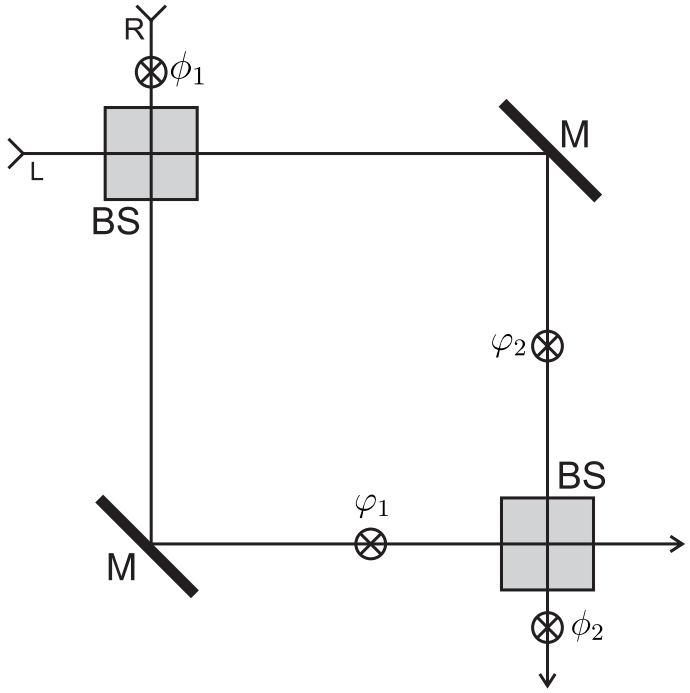

Figure 1.2: A Mach-Zehnder interferometer

The relative phase between the transmitted and reflected wave may well be controlled by a blank space as in figure 1.1. A blank space consist on a piece of material, specifically selected by its index of refraction and thickness, that retards light by changing $\vec{k}$ in that region. It can also be rotated so refraction can also play a role in the final relative phase that is gained.

In reality a BS is not reversible (it has preferred incident faces) nor symmetric and θ depends on the incident polarization and the manufacturer. Also, since the top priority in their design is the transmitted:reflected power ratio and its independence of polarization, the phases may well vary between different beam splitters.

A Mach-Zehnder (MZ) interferometer is a versatile way to manipulate momentum. From now on we shall refer to the $\vec{k}_1$ and $\vec{k}_2$ direction (figure 1.1) as the L(eft) and R(ight) path respectively. In figure 1.2 we show a MZ interferometer that consists of two 50:50 beam splitters and two mirrors (M). The parameters ϕ_1, ϕ_2, φ_1 and φ_2 are phases that can be controlled by varying the optical path-length. The zero reference is the disposition of each path such that the MZ acts as a unitary operator: in and out light have the same direction and intensity. In the present work we mount mirrors on top of a piezoelectric displacer, thus controlling the length of a path and so its acquired phase. Moving the mirror backwards makes the path longer making it accumulate a negative phase; on the other hand, moving it forward shortens the path so making the light gain a positive phase. The unitary matrix for

this operation is written as

$$U_{ph}(\theta_R, \theta_L) = \begin{pmatrix} e^{i\theta_R} & 0 \\ 0 & e^{i\theta_L} \end{pmatrix}. \tag{1.22}$$

Note that $U_p h$ refers to the path degree of freedom, in contrast to U (Eq. 1.12), which refers to polarization space. Considering the $SU(2)$ matrix of a mirror to be

$$U_{mir} = \begin{pmatrix} 0 & -i \\ -i & 0 \end{pmatrix} \tag{1.23}$$

we can obtain the unitary matrix that corresponds to the MZ interferometer in figure 1.2. Multiplying all the involved operators we obtain

$$U_{MZ} = e^{i(\phi_1+\phi_2+\varphi_1+\varphi_2)/2} \begin{pmatrix} e^{i\frac{(\phi_1+\phi_2)}{2}} \cos\left(\frac{\varphi_1-\varphi_2}{2}\right) & e^{-i\frac{(\phi_1-\phi_2)}{2}} \sin\left(\frac{\varphi_1-\varphi_2}{2}\right) \\ -e^{i\frac{(\phi_1-\phi_2)}{2}} \sin\left(\frac{\varphi_1-\varphi_2}{2}\right) & e^{-i\frac{(\phi_1+\phi_2)}{2}} \cos\left(\frac{\varphi_1-\varphi_2}{2}\right) \end{pmatrix}. \tag{1.24}$$

Ignoring the global phase, we have a $SU(2)$ matrix with $\varphi_1 - \varphi_2$, $\phi_1 + \phi_2$ and $\phi_1 - \phi_2$ as its three parameters. In this way we have total control over the evolution in momentum space, something we do not have with a single BS.

Chapter 2

Composite systems

We can always join two or more systems (subsystems) to form a larger, composite system. This is true for the classical as well as the quantum regime; however, the superposition principle gives quantum composite states a very important feature: entanglement.

Entanglement was first recognized by Einstein, Podolski and Rosen (EPR) [8] and Schrödinger [9] in the early 30's as the impossibility of writing some global states, in a composite system, as a product of its subsystem's states. This apparently simple observation started a revolution that more than 70 years later is still running [10].

Formalism establishes that every subsystem can be accessed individually. It must be possible, experimentally, to perform a unitary evolution on only one or some of the subsystems; they are distinguishable. We can conclude that a composite system can be a single quantum object with any of its degrees of freedom as subsystems [11]. In this sense and with the explanation given in chapter 1 we can consider a single photon as a composite system with its momentum and polarization degrees of freedom as subsystems.

We will now explain, in our context, the formalism of a two-qubit system and how it can be manipulated.

2.1 Two-qubit system

Hilbert spaces of subsystems are known as factor spaces. Here, we consider two qubits. Each qubit belongs to a two-dimensional factor space: the momentum or path Hilbert space $\mathcal{H}_m$ and the polarization Hilbert space $\mathcal{H}_p$. In $\mathcal{H}_m$ we have the $\{|R\rangle, |L\rangle\}$ basis so that we can write any momentum state as

$$|\psi_m\rangle = a\,|R\rangle + b\,|L\rangle \tag{2.1}$$

with a and b complex numbers. On the other hand, in $\mathcal{H}_p$ we have the $\{|H\rangle, |V\rangle\}$ basis so that we can write any polarization state (elliptical) as

$$|\psi_p\rangle = c\,|H\rangle + d\,|V\rangle \tag{2.2}$$

with c and d complex numbers.

To describe composite systems we require the product Hilbert space: the tensor product of all factor spaces involved. In our case we have $\mathcal{H} = \mathcal{H}_m \otimes \mathcal{H}_p$. In the same manner, the product of every possible pair between elements of the $\mathcal{H}_p$ and $\mathcal{H}_m$ bases is an element of the $\mathcal{H}$ basis. We identify the latter as $\{|RH\rangle, |RV\rangle, |LH\rangle, |LV\rangle\}$. We then write any bipartite state as

$$|\Psi\rangle = \alpha\,|RH\rangle + \beta\,|RV\rangle + \gamma\,|LH\rangle + \delta\,|LV\rangle \tag{2.3}$$

with α, β, γ and δ complex numbers.

The Bell basis is a useful tool to describe two-qubit states. This basis is defined by the following four states

$$\left|\Phi^+\right\rangle = \frac{1}{\sqrt{2}}(|RH\rangle + |LV\rangle) \tag{2.4a}$$

$$\left|\Phi^-\right\rangle = \frac{-i}{\sqrt{2}}(|RH\rangle - |LV\rangle) \tag{2.4b}$$

$$\left|\Psi^+\right\rangle = \frac{-i}{\sqrt{2}}(|RV\rangle + |LH\rangle) \tag{2.4c}$$

$$\left|\Psi^-\right\rangle = \frac{1}{\sqrt{2}}(|RV\rangle - |LH\rangle) \tag{2.4d}$$

Usually the first three are referred as the triplet and the last one as the singlet. We have introduced the global phase factors $(-i)$ in $|\Phi^-\rangle$ and $|\Psi^+\rangle$ for future convenience. It is easy to observe that none of the Bell states is separable: they are entangled. Actually, they are maximally entangled.

States in a bipartite system can always be written as a sum of product states that are mutually orthogonal. This is stated as a theorem.

Theorem 1 (Schmidt decomposition) *[11]*
Let $\left|\psi^{AB}\right\rangle$ be a normalized pure state of the composite system $\mathcal{S}^{AB}$ in the product Hilbert space $\mathcal{H}^{AB} = \mathcal{H}^A \otimes \mathcal{H}^B$ with $\mathtt{dim}\mathcal{H}^A = a$ and $\mathtt{dim}\mathcal{H}^B = b$. With $\rho^{AB} = \left|\psi^{AB}\right\rangle\left\langle\psi^{AB}\right|$, the operators $\rho^A = tr_B(\rho^{AB})$ and $\rho^B = tr_A(\rho^{AB})$ are the reduced density operators of the subsystems $\mathcal{S}^A$ and $\mathcal{S}^B$. Then we have the following results:

- *The vector* $\left|\psi^{AB}\right\rangle$ *can be written in the form of a Schmidt decomposition*

$$\left|\psi^{AB}\right\rangle = \sum_{n=1}^{k} \sqrt{p_n} \left|u_n^A, w_n^B\right\rangle \quad with \quad p_n \geq 0 \tag{2.5}$$

with k≤min(a,b), where $\{\left|u_n^A\right\rangle\}$ *and* $\{\left|w_n^B\right\rangle\}$ *are the orthonormalised eigenvectors of* ρ^A *in* $\mathcal{H}^A$ *(or* ρ^B *in* $\mathcal{H}^B$*) with suitably chosen phases. For pairwise differing eigenvalues* p_n *(i.e. no degeneracy), the vectors* $\left|u_n^A\right\rangle$ *and* $\left|w_n^B\right\rangle$ *are uniquely determined up to a phase. It follows from this that:*

- ρ^A *and* ρ^B *have the same positive eigenvalues* $p_1, \ldots, p_k$ *(for g-fold degeneracy, the corresponding eigenvalue is to be repeated g times).*

The number k is called the Schmidt rank of $\left|\psi^{AB}\right\rangle$*. If k>1 then the state is entangled.*

For our two-qubit system, the equation 2.5 can be written as

$$|\Psi\rangle = e^{-i\beta/2} \cos\alpha/2 \, |\mathbf{m}_1\rangle \, |\mathbf{p}_1\rangle + e^{i\beta/2} \sin\alpha/2 \, |\mathbf{m}_2\rangle \, |\mathbf{p}_2\rangle \,, \tag{2.6}$$

where $|\mathbf{m}_j\rangle$ and $\left|\mathbf{p}_j\right\rangle$ are vectors like 2.1 and 2.2 in $\mathcal{H}_m$ and $\mathcal{H}_p$ respectively such that $\langle \mathbf{m}_i | \mathbf{m}_j \rangle = \left\langle \mathbf{p}_i \middle| \mathbf{p}_j \right\rangle = \delta_{ij}$. The theorem states that any vector in $\mathcal{H}$ can always be written as the superposition of at most two particular, orthonormal separable states, even though the global state may be entangled. Whether or not $|\Psi\rangle$ is entangled is parametrized only by α. Therefore, we can think of α as being the entanglement. Indeed, $\sin(\alpha)$ equals the concurrence [12] that is a well known measure of entanglement.

2.1.1 Maximally entangled states (MES)

Maximal concurrence is achieved when $\alpha = \pi/2$; we then call these states maximally entangled. By expanding 2.6 we can conclude that MES are parametrized by two complex numbers α and β in the following way:

$$|\Psi_{ME}\rangle = \frac{1}{\sqrt{2}}(\alpha \, |RH\rangle + \beta \, |RV\rangle - \beta^* \, |LH\rangle + \alpha^* \, |LV\rangle) \tag{2.7}$$

with the constraint $|\alpha|^2 + |\beta|^2 = 1$. It will be useful later to rewrite 2.7 in the Bell basis:

$$|\Psi_M E\rangle = Re(\alpha) \left|\Phi^+\right\rangle - Im(\beta) \left|\Psi^+\right\rangle + Re(\beta) \left|\Psi^-\right\rangle - Im(\alpha) \left|\Phi^-\right\rangle . \tag{2.8}$$

2.1.2 Local, bilocal and non-local evolutions

In the same manner we did with the basis elements of $\mathcal{H}$, we can obtain its operator basis. We identify the latter as $\{\sigma_i^m \otimes \sigma_j^p\}$ $(i,j = 0,1,2,3)$ where $\sigma_0^{m,p} = \mathbb{1}_{m,p}$. We can write then any operator $\mathcal{O}$ in $\mathcal{H}$ as a sum:

$$\mathcal{O} = \sum_{i,j} a_{ij} \sigma_i^m \otimes \sigma_j^p. \tag{2.9}$$

A unitary operator U should fulfill $UU^\dagger = U^\dagger U = \mathbb{1}_m \otimes \mathbb{1}_p$.

We mentioned the separability criterion for vectors in $\mathcal{H}$ as we also mentioned that subsystems must be distinguishable. Up to this point, nothing prevent us from having a separability criterion for operators. Actually, the definition of subsystem encourages this; we must have separable unitary operators in $\mathcal{H}$. These can be of the form $U_m \otimes \mathbb{1}_p$ or $\mathbb{1}_m \otimes U_p$ known as local operators or of the form $U_m \otimes U_p$ known as bilocal operators.

Separable operators do not change entanglement. A unitary transformation will preserve orthonormality since the inner product is invariant under this type of transformations. If we now apply to 2.6 a separable unitary evolution we would realize that only the product states will change but remain orthonormal. Therefore, the Schmidt decomposition of the new state , since it is unique, will have the same α but not the same β in general; entanglement is not changed.

We have concluded that a separable unitary transformation in $\mathcal{H}$ do not change entanglement. We can rephrase this by saying that if entanglement is changed this is due to a non separable unitary transformation (non-local evolutions).

2.2 Momentum-Polarization transformation

In chapter 1 we described how polarization and momentum of light can be separately accessed, this led us to identify both degrees of freedom as subsystems in a single photon. We will now describe how can a given unitary evolution in $\mathcal{H}$ be implemented [2].

The proposal consists on inserting a QHQ set along with every ϕ_1, ϕ_2, φ_1 and φ_2 phase of figure 1.2. This way we end up with a Mach-Zehder type interferometer like in figure 2.1. In order to obtain the unitary matrix corresponding to this new array we need to introduce a new type of operator:

$$U_{mp} = e^{i\theta_R} U_R \left|R\right\rangle \left\langle R\right| + e^{i\theta_L} U_L \left|L\right\rangle \left\langle L\right| \tag{2.10}$$

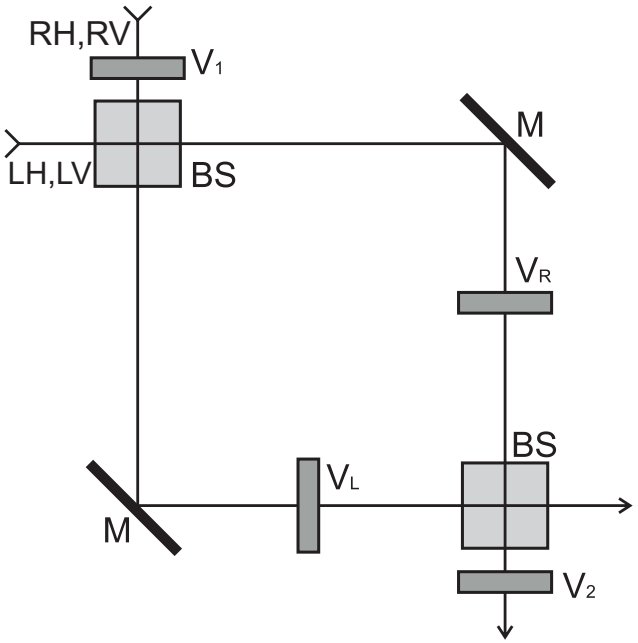

Figure 2.1: A MZ type interferometer that can perform any momentum-polarization unitary evolution

where U_R and U_L are $SU(2)$ operators acting on polarization only while $e^{i\theta_R}$ and $e^{i\theta_L}$ are accumulated phases in momentum. By looking at figure 2.1 we identify three of these operators:

$$U_1 = V_1 |R\rangle \langle R| + |L\rangle \langle L| \tag{2.11}$$

$$U_{RL} = V_R |R\rangle \langle R| + V_L |L\rangle \langle L| \tag{2.12}$$

$$U_2 = V_2 |R\rangle \langle R| + |L\rangle \langle L| \tag{2.13}$$

where V_j $(j = 1, 2, R, L)$ are $U(2)$ operators. Using the operators for the BS and mirrors introduced in chapter 1 we multiply these operators to obtain the new array unitary matrix (S):

$$S = U_2 U_{BS} U_{RL} U_{mirr} U_{BS} U_1 \tag{2.14}$$

After some manipulation we can rewrite it as

$$S = |R\rangle \langle R| S_{RR} + |L\rangle \langle L| S_{LL} + |L\rangle \langle R| S_{LR} + |R\rangle \langle L| S_{RL} \tag{2.15}$$

where the submatrices S_{ij} $(i, j = R, L)$ are given by

$$S_{RR} = \frac{1}{2} V_2 (V_R + V_L) V_1 \tag{2.16a}$$

$$S_{LL} = \frac{1}{2} (V_R + V_L) \tag{2.16b}$$

$$S_{RL} = -\frac{i}{2} V_2 (V_R - V_L) \tag{2.16c}$$

$$S_{LR} = \frac{i}{2} (V_R - V_L) V_1 \tag{2.16d}$$

It is clear that any setting of birefringent plates and accumulated phases in momentum will give some unitary operator S. In this case, the S_{ij} sub-matrices will agree with S whenever the equations below hold true. They are obtained as follows:
$S^\dagger S = \mathbb{1}$ implies

$$S_{RR}^\dagger S_{RR} + S_{LR}^\dagger S_{LR} = \mathbb{1} \tag{2.17a}$$

$$S_{RL}^\dagger S_{RL} + S_{LL}^\dagger S_{LL} = \mathbb{1} \tag{2.17b}$$

$$S_{RR}^\dagger S_{RL} + S_{LR}^\dagger S_{LL} = 0 \tag{2.17c}$$

$$S_{RL}^\dagger S_{RR} + S_{LL}^\dagger S_{LR} = 0 \tag{2.17d}$$

$S S^\dagger = \mathbb{1}$ implies

$$S_{RR} S_{RR}^\dagger + S_{RL} S_{RL}^\dagger = \mathbb{1} \tag{2.18a}$$

$$S_{LR} S_{LR}^\dagger + S_{LL} S_{LL}^\dagger = \mathbb{1} \tag{2.18b}$$

$$S_{RR} S_{LR}^\dagger + S_{RL} S_{LL}^\dagger = 0 \tag{2.18c}$$

$$S_{LR} S_{RR}^\dagger + S_{LL} S_{RL}^\dagger = 0 \tag{2.18d}$$

2.2.1 Building the array from a given unitary operator

Given a unitary operator S in $\mathcal{H}$ and 2.16, we can find the V_j operators needed to reproduce the unitary evolution S. We start from the unitarity of S and start writing the positive, hermitian operators $S_{ij} S_{ij}^\dagger$ and $S_{ij}^\dagger S_{ij}$ in their respective eigenvector bases. Because of 2.17 and 2.18 their eigenvalues can be written using $\cos^2$ and $\sin^2$.

$$S_{RR}^\dagger S_{RR} = \cos^2 \vartheta \, |\psi_1\rangle\langle\psi_1| + \cos^2 \theta \, |\psi_2\rangle\langle\psi_2| \tag{2.19a}$$

$$S_{RR} S_{RR}^\dagger = \cos^2 \vartheta \, |\bar{\psi}_1\rangle\langle\bar{\psi}_1| + \cos^2 \theta \, |\bar{\psi}_2\rangle\langle\bar{\psi}_2| \tag{2.19b}$$

$$S_{LL}^{\dagger}S_{LL} = \cos^2\vartheta\,|\chi_1\rangle\langle\chi_1| + \cos^2\theta\,|\chi_2\rangle\langle\chi_2| \tag{2.20a}$$
$$S_{LL}S_{LL}^{\dagger} = \cos^2\vartheta\,|\bar{\chi}_1\rangle\langle\bar{\chi}_1| + \cos^2\theta\,|\bar{\chi}_2\rangle\langle\bar{\chi}_2| \tag{2.20b}$$

$$S_{LR}^{\dagger}S_{LR} = \sin^2\vartheta\,|\psi_1\rangle\langle\psi_1| + \sin^2\theta\,|\psi_2\rangle\langle\psi_2| \tag{2.21a}$$
$$S_{LR}S_{LR}^{\dagger} = \sin^2\vartheta\,|\bar{\chi}_1\rangle\langle\bar{\chi}_1| + \sin^2\theta\,|\bar{\chi}_2\rangle\langle\bar{\chi}_2| \tag{2.21b}$$

$$S_{RL}^{\dagger}S_{RL} = \sin^2\vartheta\,|\chi_1\rangle\langle\chi_1| + \sin^2\theta\,|\chi_2\rangle\langle\chi_2| \tag{2.22a}$$
$$S_{RL}S_{RL}^{\dagger} = \sin^2\vartheta\,|\bar{\psi}_1\rangle\langle\bar{\psi}_1| + \sin^2\theta\,|\bar{\psi}_2\rangle\langle\bar{\psi}_2| \tag{2.22b}$$

We are now able to write every S_{ij} using the eigenvectors and eigenvalues mentioned above. By making explicit use of he phase ambiguity of the eigenvalues we obtain

$$S_{RR} = e^{i\alpha_{RR}}\cos\vartheta\,|\bar{\psi}_1\rangle\langle\psi_1| + e^{i\beta_{RR}}\cos\theta\,|\bar{\psi}_2\rangle\langle\psi_2| \tag{2.23a}$$
$$S_{LL} = e^{i\alpha_{LL}}\cos\vartheta\,|\bar{\chi}_1\rangle\langle\chi_1| + e^{i\beta_{LL}}\cos\theta\,|\bar{\chi}_2\rangle\langle\chi_2| \tag{2.23b}$$
$$S_{LR} = e^{i\alpha_{LR}}\sin\vartheta\,|\bar{\chi}_1\rangle\langle\psi_1| + e^{i\beta_{LR}}\sin\theta\,|\bar{\chi}_2\rangle\langle\psi_2| \tag{2.23c}$$
$$S_{RL} = e^{i\alpha_{RL}}\sin\vartheta\,|\bar{\psi}_1\rangle\langle\chi_1| + e^{i\beta_{RL}}\sin\theta\,|\bar{\psi}_2\rangle\langle\chi_2| \tag{2.23d}$$

The S_{ij} expressed in this way must give S. This implies the following phase relations:

$$-\alpha_{RR} + \alpha_{RL} = -\alpha_{LR} + \alpha_{LL} \pm \pi \tag{2.24}$$
$$-\beta_{RR} + \beta_{RL} = -\beta_{LR} + \beta_{LL} \pm \pi \tag{2.25}$$

By writing the submatrices as in 2.23 we must identify the α_{ij} and β_{ij} phases and the above relations will be fulfilled.

We extract from 2.16 two identities:

$$S_{LL} = V_2^{\dagger}S_{RR}V_1^{\dagger} \tag{2.26a}$$
$$S_{RL} = -V_2 S_{LR} V_1^{\dagger}. \tag{2.26b}$$

From 2.26 we obtain:

$$S_{LL}S_{LL}^{\dagger} = V_2^{\dagger}S_{RR}S_{RR}^{\dagger}V_2 \tag{2.27}$$
$$S_{LL}^{\dagger}S_{LL} = V_1 S_{RR}^{\dagger}S_{RR}V_1^{\dagger} \tag{2.28}$$

We can understand both V_1 and V_2 as basis change and write:

$$V_1 = e^{i\gamma_1}\left|\chi_1\right\rangle\!\left\langle\psi_1\right| + e^{i\Gamma_1}\left|\chi_2\right\rangle\!\left\langle\psi_2\right| \tag{2.29}$$
$$V_2 = e^{i\gamma_2}\left|\bar{\psi}_1\right\rangle\!\left\langle\bar{\chi}_1\right| + e^{i\Gamma_2}\left|\bar{\psi}_2\right\rangle\!\left\langle\bar{\chi}_2\right| \tag{2.30}$$

Considering 2.24 and 2.25 we can identify $\Gamma_{1,2}$ and $\gamma_{1,2}$:

$$\begin{aligned}
\gamma_1 = &\quad \alpha_{LR} - \alpha_{LL} & \gamma_2 = &\quad \alpha_{RR} - \alpha_{LR} \\
= &\quad \alpha_{RR} - \alpha_{RL} \pm \pi & = &\quad \alpha_{RL} - \alpha_{LL} \mp \pi \\
\Gamma_1 = &\quad \beta_{LR} - \beta_{LL} & \Gamma_2 = &\quad \beta_{RR} - \beta_{LR} \\
= &\quad \beta_{RR} - \beta_{RL} \pm \pi & = &\quad \beta_{RL} - \beta_{LL} \mp \pi
\end{aligned}$$

Let the operator $A = V_2^{\dagger}S_{RL} = -S_{LR}V_1^{\dagger}$ so that $A^{\dagger}A = S_{RL}^{\dagger}S_{RL}$. We can rewrite equation 2.17c using A and 2.26:

$$\begin{aligned}
S_{RR}^{\dagger}S_{RL} + S_{LR}^{\dagger}S_{LL} =& (V_1^{\dagger}S_{LL}^{\dagger}V_2^{\dagger})V_2 A - (V_1^{\dagger}A^{\dagger})S_{LL} \\
=& V_1^{\dagger}S_{LL}^{\dagger}A - V_1^{\dagger}A^{\dagger}S_{LL} \\
=& V_1^{\dagger}(S_{LL}^{\dagger}A - A^{\dagger}S_{LL}) \\
=& 0
\end{aligned}$$

Implying

$$S_{LL}^{\dagger}A = A^{\dagger}S_{LL} \tag{2.31}$$

Making use of 2.26 we can rewrite 2.17b

$$\begin{aligned}
\mathbb{1} =& A^{\dagger}A + S_{LL}^{\dagger}S_{LL} \\
=& A^{\dagger}A + iS_{LL}^{\dagger}A - iA^{\dagger}S_{LL} + S_{LL}^{\dagger}S_{LL} \\
=& (S_{LL}^{\dagger} - iA^{\dagger})(S_{LL} + iA) \\
\mathbb{1} =& V_R^{\dagger}V_R
\end{aligned}$$

where we have used 2.31 multiplied by i to finally obtain a unitary operator that we can identify with $V_R = S_{LL} + iA$. Multiplying instead by $-i$ we would have obtained $V_L = S_{LL} - iA$. Operating we obtain the operator A:

$$A = V_2^{\dagger}S_{RL} = -Sen\vartheta e^{i\alpha_{LL}}\left|\bar{\chi}_1\right\rangle\!\left\langle\chi_1\right| - Sen\theta e^{i\beta_{LL}}\left|\bar{\chi}_2\right\rangle\!\left\langle\chi_2\right| \tag{2.32}$$

Finally we can obtain the last two operators

$$V_R = e^{-i\vartheta} \left|\bar{\chi}_1\right\rangle\!\left\langle\chi_1\right| e^{i\alpha_{LL}} + e^{-i\theta} \left|\bar{\chi}_2\right\rangle\!\left\langle\chi_2\right| e^{i\beta_{LL}} \tag{2.33}$$

$$V_L = e^{i\vartheta} \left|\bar{\chi}_1\right\rangle\!\left\langle\chi_1\right| e^{i\alpha_{LL}} + e^{i\theta} \left|\bar{\chi}_2\right\rangle\!\left\langle\chi_2\right| e^{i\beta_{LL}} \tag{2.34}$$

Chapter 3

Holonomic phases

3.1 Pancharatnam's phase

In the early 50's, Pancharatnam [13] wanted to study the overall phase of light after having passed through some polarizers arranged in such a way that the final polarization is the same as the initial one. His objective was to verify if light that enters is in phase with the exiting light. For this, he needed to reason how to define the phase difference of two polarization states and proposed the following definition: The polarization states of any two monochromatic beams of light with the same momenta are in phase if the superposition of the two has the maximum possible intensity. Let $|\Psi_A\rangle$ and $|\Psi_B\rangle$ be two non-orthogonal states representing these beams. Then, the intensity would be given by:

$$\left(\langle\Psi_A| + \langle\Psi_B|\right)\left(|\Psi_A\rangle + |\Psi_B\rangle\right) = 2 + 2\left|\langle\Psi_A|\Psi_B\rangle\right|\cos\left(arg\left[\langle\Psi_A|\Psi_B\rangle\right]\right). \tag{3.1}$$

Following Pancharatnam's idea these two states will be in phase if $\langle\Psi_A|\Psi_B\rangle$ is real so that $arg(\langle\Psi_A|\Psi_B\rangle) = 0$. Is easy to see that this definition breaks down for orthogonal states and that we can generalize it to any pair of states regardless of its nature. We define the relative phase between two non-orthogonal states or Pancharatnam's phase as

$$\Phi_P = \Phi_{rel} = arg\left(\langle\Psi_1|\Psi_2\rangle\right) \tag{3.2}$$

Although this definition is valid for the classical as well the quantum regime, we will use it and focus only on the quantum regime from now on.

3.2 Geometric phase

Anholonomy or holonomy is the failure of certain variables, describing a system, to return to their original values. Is holonomy present in quantum theory? A first hint was given by Berry who, while studying stationary states, corrected the adiabatic theorem by introducing a new (global) phase which he called geometric phase [14]. Simon [15] proved that Berry's phase was a manifestation of holonomy in a hermitian line bundle.

The adiabatic theorem holds for slowly varying hamiltonians. It stated that eigenstates of these hamiltonians will evolve as instantaneous eigenstates multiplied by a global phase termed dynamical phase. Let $H(\mathbf{R})$ be a slowly varying hamiltonian with its set of time dependent parameters identified as $\mathbf{R}$. Assuming it has a discrete and non-degenerate spectrum we can take as the initial state the nth eigenstate at time $t = 0$: $|n, \mathbf{R}(0)\rangle$. Its evolution will then be given by

$$|\psi(t)\rangle = e^{-i\varphi_n(t)/\hbar} |n, \mathbf{R}(t)\rangle \tag{3.3}$$

where $\varphi_n(t) = \int_0^t d\tau E_n(\tau)$ is the dynamical phase and $E_n(\tau)$ is the instantenous eigenvalue of the nth eigenstate. Berry, assuming an unknown time dependent phase found out that one should add

$$\gamma_n(t) = i \int_{\mathbf{R}(0)}^{\mathbf{R}(t)} \langle n, \mathbf{R}| \nabla_{\mathbf{R}} |n, \mathbf{R}\rangle \cdot d\mathbf{R} \tag{3.4}$$

to $\varphi_n(t)/\hbar$ in order to be consistent with Schrödinger's equation. Normalization of $|n, \mathbf{R}\rangle$ guarantees that γ_n is real.

Berry's discovery, initially refered only as Berry's phase [16, 17], will soon start to mutate. A big step towards today's ubiquity of the geometric phase was made by Aharanov and Anandan [18] who proved that adiabaticity is not necessary in order to obtain a geometric phase, for this they started replacing parameter space with the projective Hilbert space. Since a ray is defined as the set of states in Hilbert space ($\mathcal{H}$) that are joined by $U(1)$ transformations we can define, in simple words, the projective Hilbert space ($\mathcal{P}$) as such where every point represents a ray. From this point of view, if we parametrize a curve in $\mathcal{H}$, denoted by $\psi(s)$, and apply to it a local gauge transformation:

$$\psi(s) \to \tilde{\psi} = e^{i\alpha(s)}\psi(s) \tag{3.5}$$

then both curves will map to the same one in $\mathcal{P}$.

Geometric phase was even more general. Samuel and Bhandari [19] not only took out the cyclic evolution premise but also proved that the evolution need not be unitary. Perhaps motivated by this rapid growth and interest on abstracting the geometric phase Mukunda and Simon [20] presented the kinematic approach to geometric phases which included Pancharatnam's idea.

Starting with the curve $|\psi(s)\rangle$ in $\mathcal{H}$, we can construct a gauge invariant term [21]:

$$\langle\psi(s_1)|\psi(s_1+N\delta s)\rangle\,\langle\psi(s_1+N\delta s)|\psi(s_1+(N-1)\delta s)\rangle\ldots\langle\psi(s_1+\delta s)|\psi(s_1)\rangle \quad (3.6)$$

Of course we shall assume $\delta s \to 0$, $N \to \infty$ and $N\delta s = s_2 - s_1$. This construction remember us of Pancharatnam's work: a starting state ($|\psi(s_1)\rangle$) is passed through several polarizers ($|\psi(s1+k\delta s)\rangle\langle\psi(s1+k\delta s)|\,, k = 1,\ldots,N$) and we wish to know the phase change at the end relative to the starting state. Then we focus on

$$\beta = arg(\langle\psi(s_1)|\psi(s_1+N\delta s)\rangle\ldots\langle\psi(s_1+\delta s)|\psi(s_1)\rangle) \quad (3.7)$$

which can be written in a more useful form:

$$\beta = arg(\langle\psi(s_1)|\psi(s_2)\rangle) - \sum_{k=0}^{N-1} arg(\langle\psi(s_1+k\delta s)|\psi(s_1+(k+1)\delta s)\rangle) \quad (3.8)$$

$$= arg(\langle\psi(s_1)|\psi(s_2)\rangle) - \sum_{k=0}^{N-1} arg(\langle\psi_k|\psi_{k+1}\rangle) \quad (3.9)$$

Noting that $\langle\psi_s|\psi_{s+\delta s}\rangle \approx 1 + \langle\psi_s|\,\frac{d}{ds}\,|\psi_s\rangle\,\delta s$ for $\delta s \ll 1$ we rewrite:

$$\beta = arg(\langle\psi(s_1)|\psi(s_2)\rangle) - arg\prod_{k=0}^{N-1}(1+\,\langle\psi_k|\dot{\psi}_k\rangle\,\delta s) \quad (3.10)$$

$$= arg(\langle\psi(s_1)|\psi(s_2)\rangle) - arg\prod_{k=0}^{N-1} e^{\langle\psi_k|\dot{\psi}_k\rangle\delta s} \quad (3.11)$$

Since $|\psi(s)\rangle$ is kept normalized in $[s_1, s_2]$ then, $\langle\psi(s)|\dot{\psi}(s)\rangle = iIm(\,\langle\psi(s)|\dot{\psi}(s)\rangle)$.

Using this we obtain:

$$\beta = arg(\langle\psi(s_1)|\psi(s_2)\rangle) - arg\left(exp\left[iIm(\sum_{k=0}^{N-1}\langle\psi_k|\dot{\psi}_k\rangle\,\delta s)\right]\right) \tag{3.12}$$

$$= arg(\langle\psi(s_1)|\psi(s_2)\rangle) - Im\left(\sum_{k=0}^{N-1}\langle\psi_k|\dot{\psi}_k\rangle\,\delta s\right) \tag{3.13}$$

$$= arg(\langle\psi(s_1)|\psi(s_2)\rangle) - Im\int_{s_1}^{s_2}\langle\psi(s)|\dot{\psi}(s)\rangle\,ds \tag{3.14}$$

The final expression for the geometric phase is usually written as

$$\Phi_G = arg(\langle\psi(s_1)|\psi(s_2)\rangle) + i\int_{s_1}^{s_2}\langle\psi(s)|\dot{\psi}(s)\rangle\,ds \tag{3.15}$$

We can think of it as being composed of two other phases

$$\Phi_P = arg(\langle\psi(s_1)|\psi(s_2)\rangle) \tag{3.16}$$

$$\Phi_{dyn} = -\,i\int_{s_1}^{s_2}\langle\psi(s)|\dot{\psi}(s)\rangle\,ds \tag{3.17}$$

that are the familiar Pancharatnam (or total) and dynamic phase respectively. This Φ_G coincides with the other definitions in being gauge invariant, parameter independent and thus defined as a function of the curve in $\mathcal{P}$ even though Φ_P and Φ_{dyn} are functions of the curve in $\mathcal{H}$. This curve in $\mathcal{P}$ is embedded or constrained by the geometry of this space.

Gauge invariance allows us to eliminate the dynamical phase. Indeed, if we choose a lift $\alpha(s)$ (see e.q. 3.5) in $\mathcal{H}$ such that

$$\alpha(s) = i\int_{s_1}^{s_2}\langle\psi(s)|\dot{\psi}(s)\rangle\,ds \tag{3.18}$$

it would result in $\Phi_G = \Phi_P$. This implies that the geometric phase is always measurable.

3.3 Topological phase

Imagine yourself positioning the tip of a pencil at some point on a Möbius strip. As you start moving the pencil (always going forward) you will be drawing some curve and you will eventually complete a loop. The difference being that the tip of the pencil ends up on the other side of the paper. You'll need to complete another loop in order to get the tip of the pencil back to its original position. This phenomenon

is an holonomy that must manifest as a global phase imparted on the wave function. However, this phase would have a different nature from the geometric one. Have you completed the loop by taking another route you would have obtained the same result.

The curvature of the projective Hilbert space affects the way you can draw different curves or loops in it. The geometric phase, being a function of this curve, will be affected by the curvature as well as by your particular choice of curve. On the other hand, a phase that does not depend on your choice of curve shall be named topological phase. This, in spirit of the branch of mathematics that studies how connected a given space is.

Any space can be decomposed into base and fiber space. These are not just simple subspaces: if the decomposition is not trivial (i.e. it is not of the form $B \times F$) we can think of a space actually becoming a set of points (base space elements) with an intrinsic structure (the fiber). This may remember us of the projective mapping (i.e. $\prod : \mathcal{H} \to \mathcal{P}$) but we should not confuse the two concepts. Fibration of a space is not mapping, but looking at it from a different perspective.

The projective Hilbert space of a single qubit can be visualized as the Bloch sphere. Indeed, it has been shown in [22] that Hopf fibrations decompose the one qubit space into a S^2 base and a S^1 fiber. Identifying the latter as the global phase indetermination we are left with S^2 (the surface of a unit sphere) as the projective Hilbert space. Since the suface of a sphere is simply connected we shouldn't expect a topological contribution to the the total phase. Since S^2 has a non trivial curvature we should expect geometric phases to appear and they have indeed been measured and extensively studied.

Hopf fibrations were also applied to the two-qubit space. The base space is S^4 and the fiber is S^3. We can parametrize the former by the following identities:

$$X_0 = \langle \sigma_z \otimes \mathbb{1} \rangle_\Psi \tag{3.19}$$

$$X_1 = \langle \sigma_x \otimes \mathbb{1} \rangle_\Psi \tag{3.20}$$

$$X_2 = \langle \sigma_y \otimes \mathbb{1} \rangle_\Psi \tag{3.21}$$

$$X_3 = Re \left\langle \hat{E} \right\rangle_\Psi \tag{3.22}$$

$$X_4 = Im \left\langle \hat{E} \right\rangle_\Psi \tag{3.23}$$

where $\hat{E} = -\hat{J}(\sigma_y \otimes \sigma_y)$ is termed the Entanglor and $\hat{J}$ is the (antilinear) conjugator whose action is taking the complex conjugate of all complex numbers involved in an expression. This same operator was introduced by Wooters in [12]. This gives us the relation $C = \sqrt{X_3^2 + X_4^2}$ for the concurrence. Let's analize two extreme cases:

1. **Separable states:** X_3 and X_4 vanish. Therefore, X_0, X_1 and X_2 parametrize S^2 that are identified with the coordinates of the Bloch sphere of one qubit. Meanwhile, the fiber is decomposed into S^2 and S^1, just like the one qubit case. Finally, the overall result is two Bloch spheres, one for each qubit, and a global phase.

2. **Maximally entangled states (MES):** Since $X_3^2 + X_4^2 = 1$ all the other parameters must vanish, as $X_0^2 + X_1^2 + X_3^2 + X_4^2 = 1$. The base space transforms into a unit circle that can be described by a normalized complex number. Multiplying 2.6 or 2.7 by a global phase $e^{i\varphi}$ we realize that, due to the conjugator, it rotates a point on the base by twice the angle φ. Only when $\varphi = 0, \pi$ does the corresponding state belong to the same fibre (i.e. maps onto the same point in the base). There is a clear two-to-one correspondence between the fibre and the base under a global phase change; introducing the two-element group $Z_2 = \{-1, 1\}$ under multiplication, we can write the MES projective Hilbert space as $S^3/Z_2 = SO(3)$.

3.3.1 Visualizing MES in the SO(3) ball

We can map the coefficients (α, β) in 2.7 to another set (a, $\vec{k}$) by the identities [25]:

$$\alpha = \cos a/2 - ik_z \sin a/2 \tag{3.24}$$

$$\beta = -(k_y + ik_x) \sin a/2 \tag{3.25}$$

where $\vec{k}$ is a unit vector and $a \in [0, \pi]$. The reason for this map is that any MES can be associated with an element of $SU(2)$ by properly arranging the coefficients:

$$U_{(\alpha,\beta)} = \begin{pmatrix} \alpha & \beta \\ -\beta^* & \alpha^* \end{pmatrix}. \tag{3.26}$$

It is known that $SU(2)$ has a difeomorphism with $SO(3)$. From the axis-angle parametrization of $SU(2)$ (see e.q. 1.10) we can identify the matrix elements and obtain the above relations.

The $SO(3)$ ball is a ball of radius π with opposite, antipodal points identified. The Bell states have particular positions in this ball (see fig. 3.1)

3.3.2 Topological phases with MES

We have shown that only a 0 or π phase factor can appear with MES. Since we know that this phase is of topological nature and due to the biconnected nature of

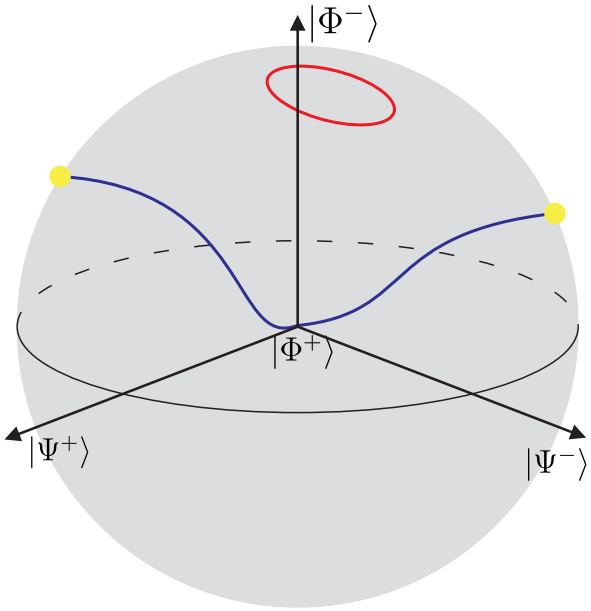

Figure 3.1: The SO(3) ball with a plus trajectory (red) and minus trajectory (blue)

$SO(3)$ [23]we can imply that there are two types of curves each one identified with a phase gain. Trajectories along which no global phase change occurs are termed "plus" and those along which there is a phase change are termed "minus"'. Every time the state crosses the space of states orthogonal to the initial one a π phase is gained; therefore we identify the "plus"' trajectories as those that make the state cross it an even number of times and the "minus"' trajectories with those that make the state cross it an odd number of times.

Chapter 4

Topological phase experiment

The main goal of the present thesis is to propose an experimental array that is able to manifest holonomic phases in a two-qubit system. To this end we will use Englert et al. [2] versatile proposal of a Mach-Zehnder type interferometer (see fig. 2.1) that can perform any local or non-local evolution on the polarization and momentum degrees of freedom of a single photon. In this way, we could study geometric as well as topological phases in the most general form possible for a two-qubit system.

In the following sections we shall describe how this experiment can be done. We start with a general point of view in order to apply it to a particular implementation aimed to exhibit the topological phase for which we present the experimental results.

4.1 Generation of entangled state in momentum and polarization

To realize any curve in projective space we need a starting point: an initial state. A Polarizing Beam Splitter (PBS) performs a non-local transformation in momentum-polarization. This type of beam splitter reflects vertically polarized states and transmits horizontally polarized one. Then, if an elliptical polarization (see eq. 2.2) is incident through the Left ($|L\rangle$) path say the resultant state would be

$$|\psi_{out}\rangle = c\,|LH\rangle + d\,|RV\rangle\,. \tag{4.1}$$

This can be rewritten as

$$|\psi_{out}\rangle = \cos\theta\,|LH\rangle + e^{i\phi}\sin\theta\,|RV\rangle\,. \tag{4.2}$$

Thus, we have obtained an entangled state. However, a PBS cannot reproduce all unitary evolutions; for example, the following transformation

$$|LH\rangle \rightarrow \frac{1}{\sqrt{2}}(|RH\rangle + |LV\rangle) \tag{4.3}$$

$$|LV\rangle \rightarrow \frac{-i}{\sqrt{2}}(|RV\rangle + |LH\rangle) \tag{4.4}$$

is impossible to implement with a PBS. We can still use it as a generator of states though. We recall equation 2.3. Reordering its coefficients we can obtain

$$|\Psi\rangle = |R\rangle (\alpha |H\rangle + \beta |V\rangle) + |L\rangle (\gamma |H\rangle + \delta |V\rangle) \tag{4.5}$$

$$= (|\alpha|^2 + |\beta|^2)^{1/2} |R\rangle \left(\frac{\alpha |H\rangle + \beta |V\rangle}{(|\alpha|^2 + |\beta|^2)^{1/2}} \right) + (|\gamma|^2 + |\delta|^2)^{1/2} |L\rangle \left(\frac{\gamma |H\rangle + \delta |V\rangle}{(|\gamma|^2 + |\delta|^2)^{1/2}} \right) \tag{4.6}$$

Which can be rewritten up to a global phase as

$$|\Psi\rangle = e^{i\phi} \sin\theta |R\rangle |\mathbf{p}_R\rangle + \cos\theta |L\rangle |\mathbf{p}_L\rangle \tag{4.7}$$

where $|\mathbf{p}_R\rangle$ and $|\mathbf{p}_L\rangle$ are two normalized but not necessarily orthogonal polarization states. It is easy to observe that this last equation is related to 4.2 by a unitary operator. Thus, submitting an elliptically polarized photon to a PBS and applying a convenient unitary evolution (QHQ) on each of the exit ports we can generate any state in the momentum-polarization Hilbert space.

Single photons, in our experiment, are generated by spontaneous parametric down conversion (SPDC) on a BBO crystal. In order to produce SPDC we excite the crystal with a 37.5 mW, 400 nm diode laser, the pump beam. SPDC generates two photons simultaneously with different momentum and frequency that are constrained, by phase matching, to the pump beam's. Then, many pairs of photons are ejected in all directions but filters on the detectors permits us only to detect photons with a wavelength of 800nm that are ejected making a 3 degree angle, each, with the pump beam line. We name one of the photons as idler if it goes directly to a detector and serves as a heralding photon while the remaining photon is named the signal and is submitted to the action of our optical array before being detected in coincidence with the idler.

We rotate the BBO crystal such that the generated photons will be vertically polarized and we identify the signal's momentum with the Left path direction. Therefore, we identify the signal's photon state as $|LV\rangle$. The initial state (after the PBS)

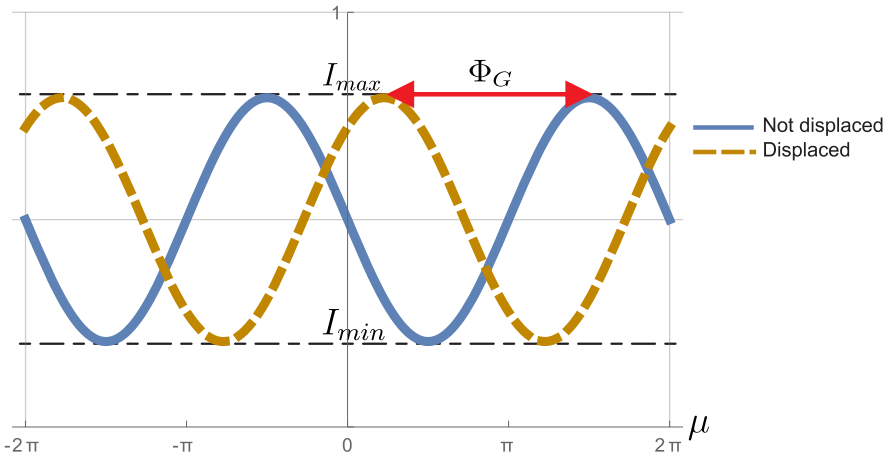

Figure 4.1: Idealized relative displacement between interferograms.

will be given by

$$|\psi_0\rangle = U_{ge}\,|LV\rangle \tag{4.8}$$

where U_{ge} is how we denote the PBS transformation.

4.2 Holonomic phase measurement

After we have generated the initial state, we must perform a unitary evolution. This evolution (U) will be performed by using Englert et al. proposal as explained in chapter 2. The resulting state will be identified with $|\psi_f\rangle$ and is given by

$$|\psi_f\rangle = U\,|\psi_0\rangle \tag{4.9}$$

$$= UU_{ge}\,|LV\rangle \tag{4.10}$$

As explained in chapter 3 the holonomic phase is measured as a relative phase between two states: $|\psi_f\rangle$ and $|\psi_0\rangle$ in the present context. We propose to measure this phase by interferometric methods. We recall that we need to measure

$$|e^{i\mu}\,|\psi_0\rangle + |\psi_f\rangle\,|^2 = 2 + 2|\,\langle\psi_0|\psi_f\rangle\,|\cos(\mu + arg(\langle\psi_0|\psi_f\rangle)) \tag{4.11}$$

where μ is a phase we have control on so it allow us to reveal an interferogram. By obtaining a zero reference interferogram (making $|\psi_f\rangle = |\psi_0\rangle$) we can obtain the holonomic phase by, after changing $|\psi_f\rangle$, measuring the relative displacement between the new interferogram and the zero reference one (see fig. 4.1).

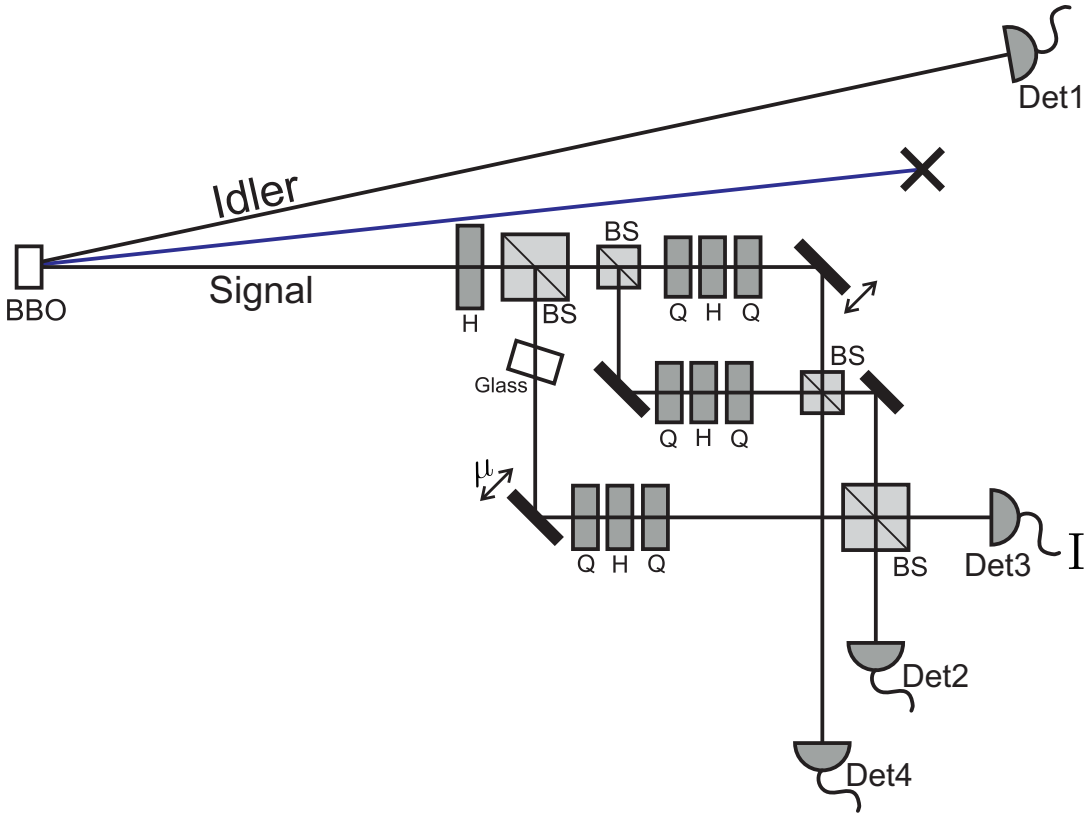

Figure 4.2: Our proposal to measure Holonomic phases in the momentum-polarization system. A Half-wave plate (H) at the beginning is used to change the initial state thus, the curve of interest. The phase reveals an interferogram that through its relative displacement permits us to measure the holonomic phase. The mirrors marked with an arrow are those which are mounted on piezoelectric translation stages.

The inner product between $|\psi_0\rangle$ and $|\psi_f\rangle$ is given by

$$\langle\psi_0|\psi_f\rangle = \langle\psi_0| U |\psi_0\rangle \tag{4.12}$$

$$= \langle LV| U_{ge}^{\dagger} U U_{ge} |LV\rangle \tag{4.13}$$

$$= \langle LV| U_{new} |LV\rangle \tag{4.14}$$

Now, we can consider U_{new} as the unitary evolution and $|LV\rangle$ as the new initial state (input state). In this way, even though $U_{new}|LV\rangle$ has two outputs (R and L) we are only interested in the L output since the initial state has that direction. We decide to obtain the interferograms with a MZ interferometer as in figure 4.2 where U_{new} is implemented by a single MZ. We do not include the PBS, the U and the $U_{ge}^{\dagger}$ implementation since placing all elements in line will involve bigger fluctuations, more instability and, thus, large experimental errors.

4.2.1 Topological phase measurement

We implemented a particular array to exhibit topological phases. We chose our initial state to be parametrized by and angle a_0 written as

$$|in\rangle = \cos(a_0/2)\left|\Phi^+\right\rangle + \sin(a_0/2)\left|\Psi^+\right\rangle \tag{4.15}$$

In this way the initial state will be located along the x axis in the $SO(3)$ ball. For this to be accomplished, we need U_{ge} to perform the following transformation

$$|RH\rangle \to \left|\Phi^-\right\rangle \tag{4.16}$$
$$|RV\rangle \to \left|\Psi^-\right\rangle \tag{4.17}$$
$$|LH\rangle \to \left|\Phi^+\right\rangle \tag{4.18}$$
$$|LV\rangle \to \left|\Psi^+\right\rangle \tag{4.19}$$

where the first two relations are chosen so that $Det(U_{ge}) = 1$. This way, the input state must be

$$|in\rangle = \cos(a_0/2)\,|LH\rangle + \sin(a_0/2)\,|LV\rangle \tag{4.20}$$

which can be accomplished with the aid of a Half-wave plate $H(\pi/2 - a_0/4)$. This retarder appears in figure 4.2 before the first BS.

In order to study topological phases the evolution U must be local. For the present work we choose the following

$$U = e^{-i\Lambda\sigma_3} \otimes e^{-i2\Lambda\sigma_2} \tag{4.21}$$

where Λ is the parameter of the curve. As will be shown next, this choice simplifies the array.

As defined before, we have $U_{new} = U_{gen}^\dagger U U_{gen}$. From the matrix representation of this operator we obtain

$$S_{LL}^\dagger S_{LL} = \cos^2(\Lambda)\,|\chi_1\rangle\langle\chi_1| + \cos^2(3\Lambda)\,|\chi_2\rangle\langle\chi_2| \tag{4.22}$$
$$S_{LL} S_{LL}^\dagger = \cos^2(\Lambda)\,|\bar{\chi}_1\rangle\langle\bar{\chi}_1| + \cos^2(3\Lambda)\,|\bar{\chi}_2\rangle\langle\bar{\chi}_2| \tag{4.23}$$

where $\Lambda = \vartheta$, $3\Lambda = \theta$ and the eigenvectors

$$|\chi_1\rangle = \frac{1}{\sqrt{2}}|H\rangle + \frac{1}{\sqrt{2}}|V\rangle = |D\rangle \tag{4.24}$$

$$|\chi_2\rangle = -\frac{1}{\sqrt{2}}|H\rangle + \frac{1}{\sqrt{2}}|V\rangle = |A\rangle \tag{4.25}$$

$$|\bar{\chi}_1\rangle = |\chi_1\rangle \tag{4.26}$$

$$|\bar{\chi}_2\rangle = |\chi_2\rangle \tag{4.27}$$

we can also obtain S_{LL}

$$S_{LL} = \begin{pmatrix} \cos(\Lambda)Cos(2\Lambda) & \sin(\Lambda)\sin(2\Lambda) \\ \sin(\Lambda)\sin(2\Lambda) & \cos(\Lambda)\cos(2\Lambda) \end{pmatrix} \tag{4.28}$$

and because of $S_{LL}|D\rangle = \cos(\Lambda)|D\rangle$, $S_{LL}|A\rangle = \cos(3\Lambda)|A\rangle$ and equation 2.23 we can conclude that $\alpha_{LL} = \beta_{LL} = 0$. Therefore we have

$$V_R = e^{-i\Lambda}|D\rangle\langle D| + e^{-i3\Lambda}|A\rangle\langle A| = e^{-2i\Lambda}(e^{i\Lambda}|D\rangle\langle D| + e^{-i\Lambda}|A\rangle\langle A|) \tag{4.29}$$

$$V_L = e^{i\Lambda}|D\rangle\langle D| + e^{i3\Lambda}|A\rangle\langle A| = e^{2i\Lambda}(e^{-i\Lambda}|D\rangle\langle D| + e^{i\Lambda}|A\rangle\langle A|) \tag{4.30}$$

is easy to note that $V_L = V_R^\dagger$ or $V_L = V_R(-\Lambda)$.

It can be shown that

$$Q(\pi/4)H(-\pi/4 + \Lambda/2)Q(\pi/4) = \begin{pmatrix} e^{i\Lambda} & 0 \\ 0 & e^{-i\Lambda} \end{pmatrix}. \tag{4.31}$$

Therefore we can calculate V_R by applying a proper rotation ($H(\pi/8)$) to 4.31

$$V_R = H(\pi/8)Q(\pi/4)H(-\pi/4 + \Lambda/2)Q(\pi/4)H(5\pi/8) \tag{4.32}$$

$$= H(\pi/8)Q(\pi/4)H(-\pi/4 + \Lambda/2)H(5\pi/8)Q(\pi) \tag{4.33}$$

$$= H(\pi/8)Q(3\pi/4)H(5\pi/8 - \Lambda/2)Q(\pi) \tag{4.34}$$

$$= Q(\pi/2)H(\pi/8)H(5\pi/8 - \Lambda/2)Q(\pi) \tag{4.35}$$

$$= Q(\pi)H(\pi/2 - \Lambda/2)Q(\pi) \tag{4.36}$$

$$= Q(0)H(\pi/2 - \Lambda/2)Q(0) \tag{4.37}$$

where we have used the properties mentioned in chapter 1. The final results are

$$V_R = e^{-2i\Lambda}Q(0)H(\pi/2 - \Lambda/2)Q(0) \tag{4.38}$$

$$V_L = e^{2i\Lambda}Q(0)H(\pi/2 + \Lambda/2)Q(0) \tag{4.39}$$

Because of the design of our array we do not need to calculate V_1 and V_2.

According to the above results, we have to modify the length of both arms of the inner MZ. We need to take into account the fact that we have only the R path mirror mounted on a piezo translator. From 2.16 we note that $V_R \pm V_L$ shows up in every S_{ij} expression, if we extract the phase from V_L then we obtain

$$U_{Englert} = e^{i2\Lambda} U_{array} \tag{4.40}$$

where U_{array} is the actual unitary operator the inner MZ is performing. We will thus carry a $e^{-i2\Lambda}$ phase we do not need; to overcome this situation we change μ to $\mu - 2\Lambda$.

4.3 Experimental procedures

We use a Mach-Zehnder type interferometer nested within another one. In the outer arm we place a blank space which is nothing more than a piece of common glass 18.6mm thick and with index of refraction of approximately 1.53. It is intended to equalize the optical path length with the inner arm that passes through two small (10mm each) beam splitters. Similarly, the retarder plates in the outer arm compensate the passage of the inner one through the same type of retarders.

Both inside and outside mirrors marked by an arrow in figure 4.2 are mounted in a piezoelectric translation stage. These piezos have an accuracy of 0.01 Volts which equals to a translation of approximately $\lambda/177$.

For the initial state we chose $a_0 = \pi$, this will make a vertical polarization enter the array. It is a better choice to let a vertical or horizontal polarization enter the array since the mirrors and beam splitters are not ideal. They behave differently depending on polarization: Indeed, polarization-dependent reflectance and phase shifts can change visibility of the interferogram but, most importantly, they may shift the pattern.

We chose to measure 4 values of Λ. To select these points we calculated the inner product $\langle \psi_0 | \psi_f \rangle$. A plot of this function is shown in figure 4.3. Every time the curve crosses the horizontal axis there is a π phase shift. Since the absolute value of this function will be the visibility, we choose those with a greater value; these are tagged by red points in figure 4.3. The four points correspond to $\Lambda = 0, \theta, \pi - \theta, \pi$ where $\theta = ArcTan(\sqrt{5}) \approx 1.15$.

For each point there is an interference pattern. This pattern shows up in the form of a signal of coincidence counts between detector 1 and detector 3 (see figure 4.2). In the ideal case, for a given Λ and varying μ we should obtain the normalized

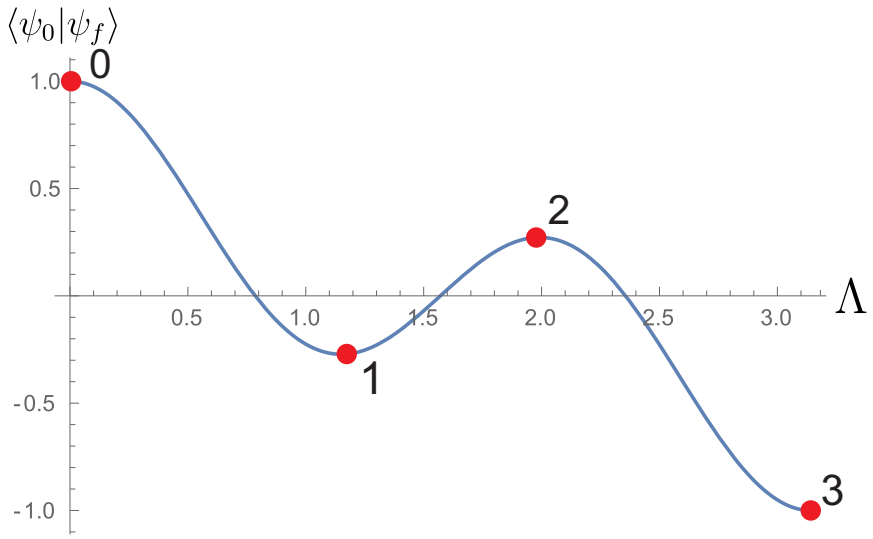

Figure 4.3: The chosen points are tagged by numbers and by red points.

signal:

$$I = 1/4(1 + 1/2(1 + \cos(2\Lambda)Cos(4\Lambda)) + 2\cos(\Lambda)\cos(2\Lambda)\cos(\mu)) \tag{4.41}$$

Ideal normalized signals are shown in figure 4.4 for the first two Λ values. Data were taken for these two Λ values. μ was fixed for 10 equally spaced values, every $2\pi/9$. Plots of the normalized data are shown in figure 4.5 and 4.6 for the first ($\Lambda = 0$) and the second ($\Lambda = \theta \approx 1.15$) points respectively.

These curves do not exactly match the expected ones from figure 4.4. We argue that this is because beam splitters are not exactly 50:50 nor they are equal, the glass may absorb too much making one arm carry a less intense beam than the other, one or more mirrors may not be working properly or bad alignment. All these error sources disturb the final signal. The final signal can be modelled by an expression of the form (see eq.3.1):

$$a + b\cos\phi \tag{4.42}$$

We can identify a and b in the ideal signal. In order to take into account any kind of error, we should multiply these ideal coefficients by a different factor (say c_a and c_b) and then find the best fit for these that will best reproduce the experimental curve. For the $\Lambda = 0$ curve we obtained $c_a = 0.88466$ and $c_b = 0.513313$ whereas for the other one we have $c_a = 0.818608$ and $c_b = 0.826093$.

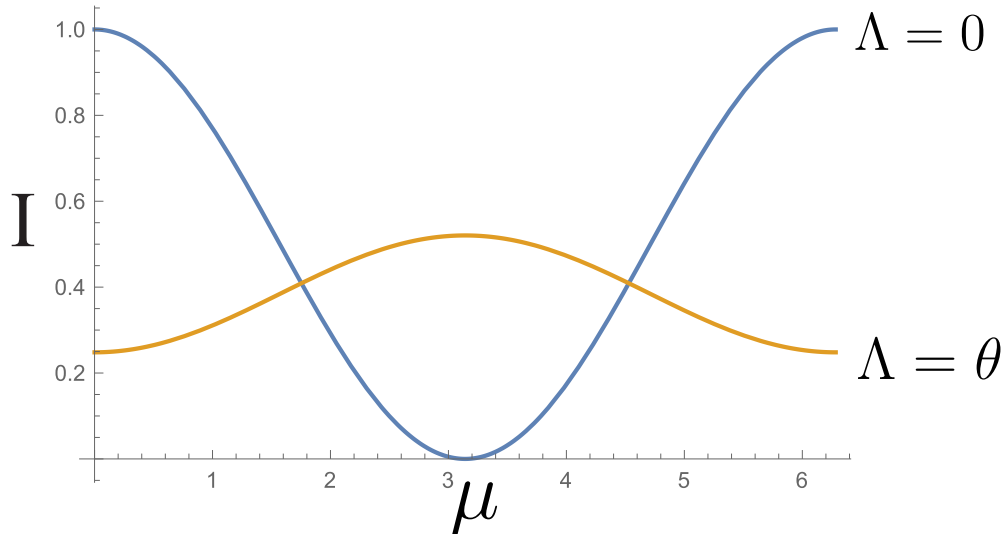

Figure 4.4: Ideal normalized signals for the first two points.

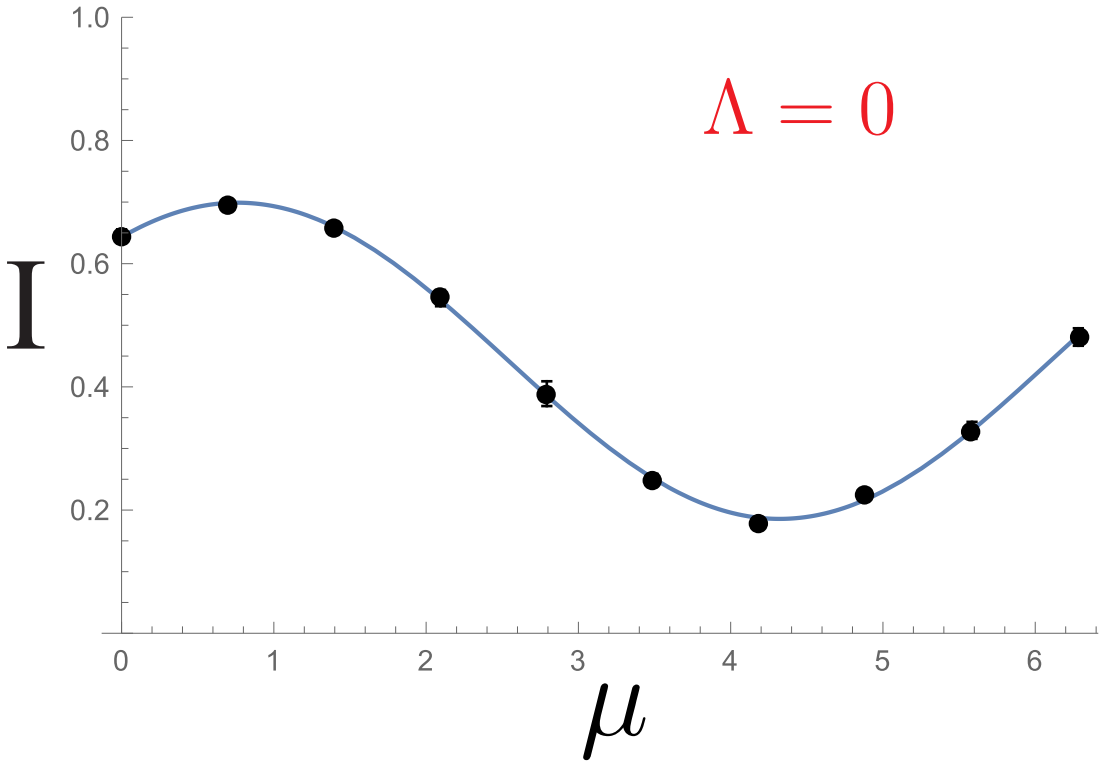

Figure 4.5: Normalized coincidence counts for the first point

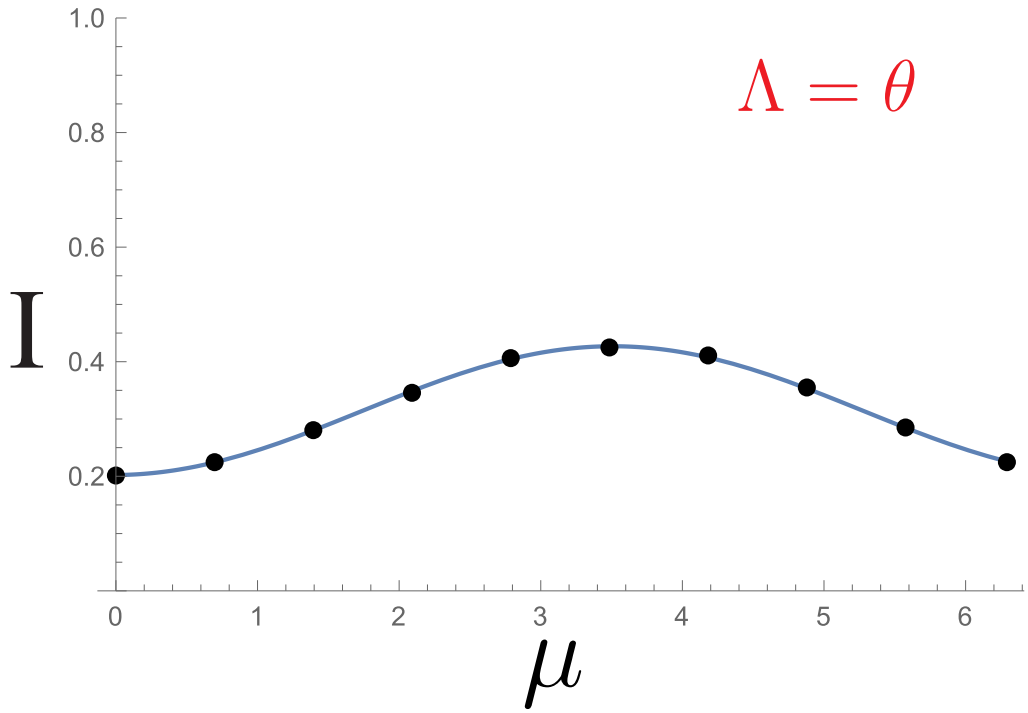

Figure 4.6: Normalized coincidence counts for the second point

Chapter 5

Summary and conclusions

This thesis work deals with an experimental array that can be used to study geometric as well as topological phases in a two-qubit system. In chapter 1 we show that is possible to perform any unitary evolution in both polarization as well as momentum independently of one another. This serves us to justify that a system composed by these two degrees of freedom of a single photon can be used as a truly two-qubit system. Chapter 2 presented a Mach-Zehnder type interferometer, a proposal by Englert et al., that can perform any type of evolution in this system, be it local or non-local evolutions.

A very interesting phenomenon in quantum theory, but that can also be exhibited in classical systems, is holonomy. In particular, in quantum theory this shows up as a global phase multiplying the wave function. Chapter 3 introduce this phenomenon by stating that the global or Pancharatnam's phase can involve three different phases, each one with a different nature: the dynamical phase depends on the Hamiltonian; the geometric phase depends on the geometry (the curvature) of the so called projective space and the topological phase responds only to the topology of it.

We have designed an experiment that, by taking advantage of the versatility of the arrangement proposed by Englert et al., can be used to study holonomic phases. We propose two nested Mach-Zehnder interferometers, in one arm we built Englert et al. arrangement (the evolution) and the other one is used as a reference to measure the holonomic phase gained by measuring relative displacements between the different measured patterns. Finally, we implemented the experiment aiming to exhibit the topological phase. Our measurements show good agreement with the expected results, considering error sources.

This work can be extended to study holonomic phases under non-local unitary evolutions.

Bibliography

[1] E. Sjöqvist, *Geometric phase for entangled spin pairs*, Phys. Rev. A **62** (2000), 022109.

[2] B.-G. Englert, C. Kurtsiefer, and H. Weinfurter, *Universal unitary gate for single-photon two-qubit states*, Phys. Rev. A **63** (2001), 032303.

[3] J. C. Loredo, M. A. Broome, D. H. Smith, and A. G. White, *Observation of entanglement-dependent two-particle holonomic phase*, Phys. Rev. Lett. **112** (2014), 143603.

[4] C. E. R. Souza, J. A. O. Huguenin, P. Milman, and A. Z. Khoury, *Topological phase for spin-orbit transformations on a laser beam*, Phys. Rev. Lett. **99** (2007), 160401.

[5] C. E. R. Souza, J. A. O. Huguenin, and A. Z. Khoury, *Topological phase structure of vector vortex beams*, J. Opt. Soc. Am. A **31** (2014), 1007–1012.

[6] J. Du, J. Zhu, M. Shi, X. Peng, and D. Suter, *Experimental observation of a topological phase in the maximally entangled state of a pair of qubits*, Phys. Rev. A **76** (2007), 042121.

[7] B. N. Simon, C. M. Chandrashekar, and S. Simon, *Hamilton's turns as a visual tool kit for designing single-qubit unitary gates*, Phys. Rev. A **85** (2012), 022323.

[8] A. Einstein, B. Podolsky, and N. Rosen, *Can quantum-mechanical description of physical reality be considered complete?*, Phys. Rev. **47** (1935), 777–780.

[9] E. Schrödinger, *Die gegenwärtige situation in der quantenmechanik*, Naturwissenschaften **23** (1935), 807–812.

[10] R. Horodecki, P. Horodecki, M. Horodecki, and K. Horodecki, *Quantum entanglement*, Rev. Mod. Phys. **81** (2009), 865–942.

[11] J. Audretsch, *Entangled Systems: New Directions in Quantum Physics*, Wiley-VCH, 2007.

[12] W. K. Wootters, *Entanglement of formation of an arbitrary state of two qubits*, Phys. Rev. Lett. **80** (1998), 2245–2248.

[13] S. Pancharatnam, *Generalized theory of interference, and its applications*, Proc. Indian Acad. Sci. A **44** (1956), 247–262.

[14] M. V. Berry, *Quantal phase factors accompanying adiabatic changes*, Proceedings of the Royal Society of London. Series A, Mathematical and physical sciences **392** (1984), 45–57.

[15] B. Simon, *Holonomy, the quantum adiabatic theorem, and berry's phase*, Phys. Rev. Lett. **51** (1983), 2167–2170.

[16] A. Tomita and R. Y. Chiao, *Observation of berry's topological phase by use of an optical fiber*, Phys. Rev. Lett. **57** (1986), 937–940.

[17] T. Bitter and D. Dubbers, *Manifestation of berry's topological phase in neutron spin rotation*, Phys. Rev. Lett. **59** (1987), 251–254.

[18] Y. Aharonov and J. Anandan, *Phase change during a cyclic quantum evolution*, Phys. Rev. Lett. **58** (1987), 1593–1596.

[19] J. Samuel and R. Bhandari, *General setting for berry's phase*, Phys. Rev. Lett. **60** (1988), 2339–2342.

[20] N. Mukunda and R.Simon, *Quantum kinematic approach to the geometric phase. i. general formalism*, Annals of Physics **228** (1993), 205–268.

[21] V. Bargmann, *Note on wigner's theorem on symmetry operations*, J. Math. Phys. **5** (1964), 862–868.

[22] R. Mosseri and R. Dandoloff, *Geometry of entangled states, bloch spheres and hopf fibrations*, Journal of Physics A: Mathematical and General **34** (2001), 10243.

[23] P. Milman, *Phase dynamics of entangled qubits*, Phys. Rev. A **73** (2006), 062118.

[24] P. Milman and R. Mosseri, *Topological phase for entangled two-qubit states*, Phys. Rev. Lett. **90** (2003), 230403.

[25] W. LiMing, Z. L. Tang, and C. J. Liao, *Representation of the* SO(3) *group by a maximally entangled state*, Phys. Rev. A **69** (2004), 064301.